## High temperature conductance characteristics of $LaAlO_3/SrTiO_3$ -heterostructures under equilibrium oxygen atmospheres

F. Gunkel, S. Hoffmann-Eifert, R. Dittmann, S. B. Mi, C. L. Jia, P. Meuffels, and R. Waser

Citation: Appl. Phys. Lett. 97, 012103 (2010); doi: 10.1063/1.3457386

View online: https://doi.org/10.1063/1.3457386

View Table of Contents: http://aip.scitation.org/toc/apl/97/1

Published by the American Institute of Physics

## Articles you may be interested in

Influence of charge compensation mechanisms on the sheet electron density at conducting LaAlO<sub>3</sub>/SrTiO<sub>3</sub>-interfaces

Applied Physics Letters 100, 052103 (2012); 10.1063/1.3679139

Perovskite substrates boost the thermopower of cobaltate thin films at high temperatures Applied Physics Letters **110**, 253101 (2017); 10.1063/1.4986778

Defects and transport in complex oxide thin films

Journal of Applied Physics 103, 103703 (2008); 10.1063/1.2921972

Quasi-ideal strontium titanate crystal surfaces through formation of strontium hydroxide Applied Physics Letters **73**, 2920 (1998); 10.1063/1.122630

Stoichiometry control of the electronic properties of the LaAlO<sub>3</sub>/SrTiO<sub>3</sub> heterointerface Applied Physics Letters **102**, 251602 (2013); 10.1063/1.4812353

Stoichiometry dependence and thermal stability of conducting NdGaO<sub>3</sub>/SrTiO<sub>3</sub> heterointerfaces Applied Physics Letters **102**, 071601 (2013); 10.1063/1.4792509



## High temperature conductance characteristics of LaAlO<sub>3</sub>/SrTiO<sub>3</sub>-heterostructures under equilibrium oxygen atmospheres

F. Gunkel, <sup>1,2,a)</sup> S. Hoffmann-Eifert, <sup>1,2</sup> R. Dittmann, <sup>1,2</sup> S. B. Mi, <sup>2,3</sup> C. L. Jia, <sup>2,3</sup> P. Meuffels, <sup>1,2</sup> and R. Waser<sup>1,2</sup>

(Received 26 March 2010; accepted 5 June 2010; published online 7 July 2010)

The interface conductance of LaAlO<sub>3</sub>/SrTiO<sub>3</sub> heterostructures was investigated under high temperature oxygen equilibrium. The dependence of the heterostructure's conductance on oxygen partial pressure (from 10<sup>-22</sup> to 1 bar) and temperature (800 to 1100 K) was compared to the characteristic of SrTiO<sub>3</sub> single crystals, which is described in terms of a defect chemistry model. Up to 950 K the equilibrated heterostructures reveal an additional influence of a metallic-like conduction path with a very slight dependence on the oxygen partial pressure. Donor-type interface states which may result from either lattice distortions or A-site cation intermixing during processing are discussed as a possible origin for the exceptional interface conduction of LaAlO<sub>3</sub>/SrTiO<sub>3</sub> heterostructures. © 2010 American Institute of Physics. [doi:10.1063/1.3457386]

The discovery of the highly conducting interface between LaAlO<sub>3</sub> (LAO) films and SrTiO<sub>3</sub> (STO) substrates has led to miscellaneous studies on the fundamental structural and electrical properties of LAO/STO-heterostructures grown by pulsed laser deposition (PLD) and has evoked extensive discussions about the physical mechanisms which underlie the high concentration of charge carriers in the interface region  $(10^{13}-10^{17}~{\rm cm}^{-2})$ . L2

In analogy to the formation of a two-dimensional electron gas in polar semiconductor heterointerfaces it was proposed that a polarity discontinuity at the atomically abrupt interface between LAO and STO causes an electronic reconstruction resulting in a conducting interface. 1-3 However, due to the complex interplay between defect chemistry and electrical conductivity of STO, an increase in the electronic charge carrier concentration in the substrate itself has also been taken into account. The effects under discussion include the generation of oxygen vacancies<sup>4,5</sup> and a possible A-site lanthanum doping<sup>3,6,7</sup> in the STO substrate resulting from the high energetic impingement of the incoming particles during the PLD process. In this context, a strong impact of the oxygen atmosphere during PLD growth on the low temperature conductivity of LAO/STO-heterostructures with undefined defect configuration has been observed but no studies of the interface conductivity under equilibrium conditions have been reported so far.

It is known that the oxygen sublattice of STO can reach equilibrium with the surrounding oxygen atmosphere at temperatures above 750 K. Therefore, we performed *in situ* measurements of the high temperature conductance (HTC) of LAO/STO-heterostructures in controlled oxygen partial pressure in order to gain more detailed insight into the defect structure of the LAO/STO-interface.

The samples were prepared by growing 8 unit cells of LAO on  ${\rm TiO_2}$ -terminated (100)-STO-substrates by means of PLD at a temperature of 970 K and a deposition oxygen pressure of  $4\times10^{-5}$  mbar. Clear reflection high energy electron diffraction intensity oscillations were observed during the process indicating layer-by-layer growth mode. When exceeding a layer thickness of 4 unit cells, conducting interfaces were obtained after cooling down the samples to room temperature under deposition pressure. Those samples exhibited a sheet conductance of about 0.03 mS at 300 K as determined by four-point-probe measurements in a van der Pauw configuration. The conductances of the as-deposited heterostructures showed a metallic-like low temperature behavior as presented in Fig. 3(a), consistent with the report of Brinkman *et al.*<sup>8</sup>

The perfect crystallinity and the epitaxial character of the thin films were verified by high-resolution (scanning) transmission electron microscopy. Figure 2(d) shows an high angle annular dark field (HAADF) image of an interface region of a representative, as-grown sample. Under the HAADF conditions the atomic columns give rise to bright contrast and the intensity of the image maxima increases with atomic number from AlO columns via TiO, Sr to La columns. Thus, the distinct features in Fig. 2(d) originate mainly from the A-site columns of the STO substrate (bottom) and the LAO layer (top). The brightness across the interface shows rather a gradual decrease than an abrupt, step-like change demonstrating A-site cation intermixing on a length scale of 2–3 unit cells at the interface in agreement with the findings of Nakagawa *et al.*<sup>3</sup>

The HTC measurements were performed at temperatures between 820 and 1250 K in an yttria-stabilized zirconia oxygen-pump system which allowed to continuously adjust the oxygen partial pressure (pO<sub>2</sub>) between 1 and  $10^{-22}$  bar (for more details it is referred to Ohly *et al.* <sup>10</sup>). The setup was equipped with a triaxially shielded four-point-probe system

<sup>&</sup>lt;sup>1</sup>Institute of Solid State Research, Electronic Materials, Forschungszentrum Juelich, 52425 Juelich, Germany

<sup>&</sup>lt;sup>2</sup>JARA-Fundamentals of Future Information Technology, Forschungszentrum Juelich, 52425 Juelich, Germany

<sup>&</sup>lt;sup>3</sup>Institute of Solid State Research, Ernst-Ruska Centre for Microscopy and Spectroscopy with Electrons, Forschungszentrum Juelich, 52425 Juelich, Germany

<sup>&</sup>lt;sup>a)</sup>Electronic mail: f.gunkel@fz-juelich.de.

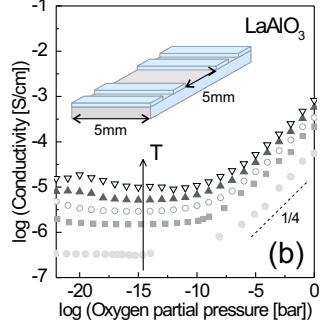


FIG. 1. (Color online) Reference measurements on a STO single crystal (a) and a LAO single crystal (b) vs  $pO_2$  in a double logarithmic plot measured at various temperatures: 1100 K  $(\nabla)$ , 1050 K  $(\blacktriangle)$ , 1000 K  $(\bigcirc)$ , 950 K  $(\blacksquare)$ , and 850 K  $(\blacksquare)$ . Inset: schematic illustration of the sample geometry.

for the electrical characterization. Electrical contact to the  $5 \times 10 \times 0.5$  mm<sup>3</sup>-wide samples was achieved by four sputtered Pt-electrodes whereas the inner electrodes were spaced 5 mm apart from each other [see inset of Fig. 1(b)].

Figure 1 presents the HTC reference measurements of a STO single crystal substrate and a LAO single crystal, respectively. The conductivity of STO varies over many orders of magnitude due to its extreme sensitivity to the defect concentrations within the crystal which are related to the ambient pO<sub>2</sub> via defect equilibria. <sup>11,12</sup> In the low pO<sub>2</sub>-regime STO shows n-type conductivity as a result of the oxygen loss which gives rise to the generation of free electrons. In oxygen rich atmospheres, p-type conductivity is observed due to the creation of free holes when incorporating oxygen into the crystal. The underlying oxygen exchange reactions in Kroeger–Vink notation read

Reduction: 
$$O_0^x \rightleftharpoons 1/2O_2 + V_0^{\bullet \bullet} + 2e'$$
, (1)

Oxidation: 
$$V_0^{\bullet \bullet} + 1/2O_2 \rightleftharpoons O_0^x + 2h^{\bullet}$$
. (2)

From these defect chemical reactions, the characteristic slopes of (-1/4) and (+1/4) observed in the pO<sub>2</sub>dependence of the conductivity can be deduced for STO with inherent acceptor-type impurity content. 11 The deviations in the intermediate pO<sub>2</sub>-regime between electronic conductivity denoted by the solid lines and measured data points are attributed to the ionic conductivity contribution due to oxygen vacancy diffusion. The conductivity of the LAO single crystal [Fig. 1(b)] can likewise be ascribed to hole conduction following a (+1/4)-dependence in the oxidizing regime and a constant ionic conductivity contribution under reducing atmospheres. 13 The mixed ionic electronic conduction characteristic of the two materials allows that an equilibrium of the entire oxygen sublattice of the LAO/STO-heterostructure with the surrounding atmosphere was established in the studied temperature range. In particular, the epitaxial LAO layer does not work as a barrier for oxygen diffusion above 800 K.

The results of HTC measurements of a LAO/STO-heterostructure under controlled oxygen atmosphere are illustrated in Figs. 2(a)–2(c) in comparison to the bare STO single crystal. In a simple model the dc characteristic of the heterostructure can be described by the sum of three parallel conductance contributions  $G_{\rm STO}$ ,  $G_{\rm IF}$ , and  $G_{\rm LAO}$  corresponding to STO single crystal, metallic interface, and LAO layer. Since the STO-substrate exceeds the thickness of the LAO thin film by a factor of  $10^4$ , one can deduce from the refer-

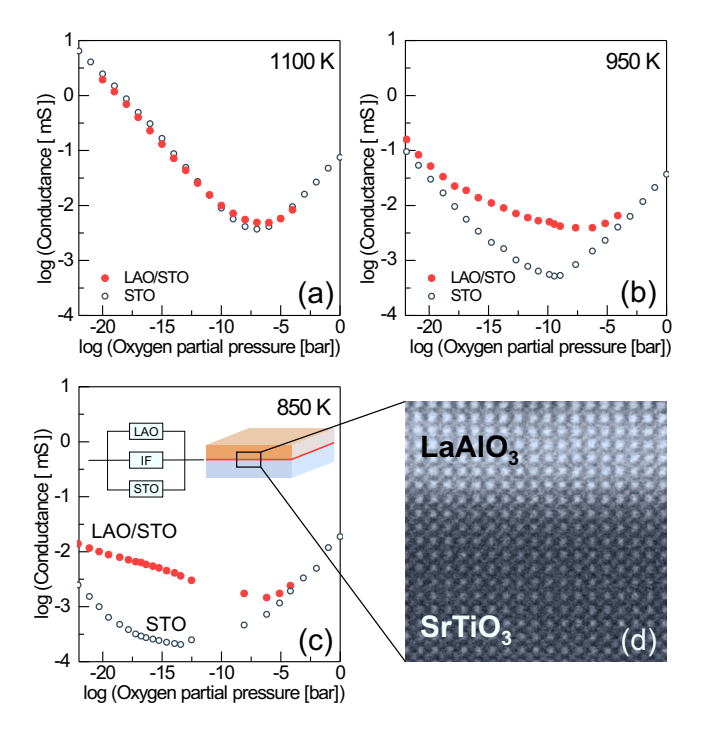


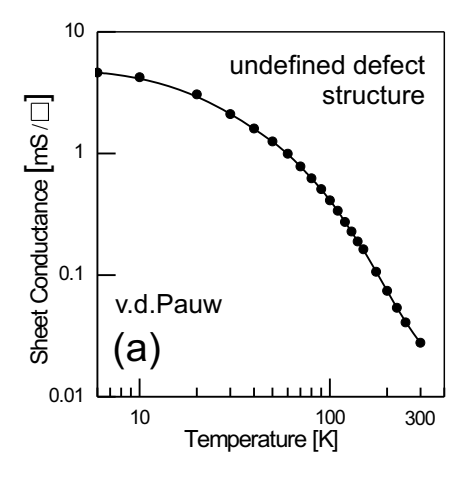
FIG. 2. (Color) [(a)-(c)] HTC characteristics of a LAO/STO-heterostructure (red, filled circles) and a STO single crystal (open circles) in equilibrium with the surrounding pO<sub>2</sub> measured at different temperatures. (d) HAADF image of the LAO/STO-interface region in an as-grown sample.

ence measurements that the film contribution is always small compared to the substrate contribution and can be neglected. The total conductance of the heterostructure  $G_{\rm tot}$  is then given by

$$G_{\text{tot}} = G_{\text{IF}} + G_{\text{STO}} + G_{\text{LAO}} \approx G_{\text{IF}} + G_{\text{STO}}.$$
 (3)

At 1100 K [Fig. 2(a)]  $G_{\rm tot}$  is completely governed by the STO-substrate contribution  $G_{STO}$  over the entire pO<sub>2</sub>-range. Therefore, no statements concerning the interface conductance  $G_{\rm IF}$  are possible at temperatures of 1100 K and higher. At lower temperatures, however, clear deviations between the conductance characteristic of the heterostructure and the single crystal are observed in the range  $10^{-18}$  bar  $\leq$  pO<sub>2</sub>  $\leq 10^{-5}$  bar [Figs. 2(b) and 2(c)]. Here, the total conductance  $G_{\rm tot}$  is strongly affected by the interface contribution  $G_{\rm IF}$ while it still remains dominated by the substrate contribution outside this pressure range. Hence, reliable values for  $G_{IF}$ can only be extracted up to a temperature of 950 K before the interface contribution is concealed by the increasing substrate contribution. For the given temperature and pO2 range it can be deduced that  $G_{\rm IF}$  possesses a very weak  $pO_2$ -dependence far beyond the  $(\pm 1/4)$ -dependence of the STO single crystal.

The temperature dependence of the heterostructure's conductance measured under controlled  $pO_2=10^{-18}$  bar is analyzed in more detail in Fig. 3(b). Two temperature regimes can be distinguished: from 820 to 900 K  $G_{tot}$  (black circles) decreases with increasing temperature down to a value of about 0.01 mS possessing to a metallic-type behavior. Above 900 K,  $G_{tot}$  increases with increasing temperature due to the exponentially rising conductance of the STO substrate. Hence, the decrease in the total conductance below 900 K has to be attributed to the interface contribution according to Eq. (3). This remarkable result indicates that the interface still exhibits a metallic-like conductance at



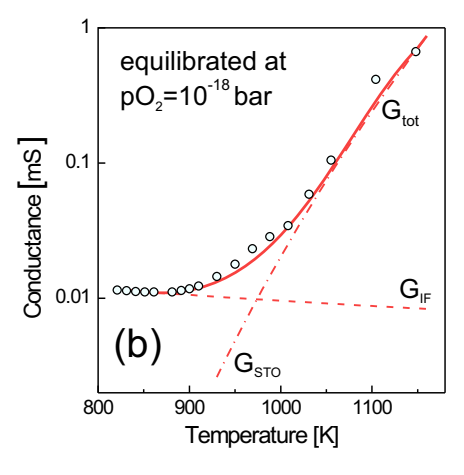


FIG. 3. (Color) (a) Low temperature sheet conductance of an as-grown LAO/STO-heterostructure measured in a van der Pauw configuration. (b) Temperature dependence of the heterostructure's conductance equilibrated at  $pO_2=10^{-18}$  bar. Expt. data ( $\bigcirc$ ); fits: metallic interface contribution  $G_{\rm IF} \simeq 1/T$  (-), substrate contribution  $G_{\rm STO} \simeq \exp\{-E_A/k_{\rm B}T\}$  (-), and total conductance  $G_{\rm tot} = G_{\rm STO} + G_{\rm IF}$  (-).

900 K under equilibrium conditions. As a very good approximation, the total conductance (solid red line) can finally be represented by the sum of the metallic interface contribution,  $G_{\rm IF}^{\,\,} \simeq 1/T$ , and the substrate contribution,  $G_{\rm STO}^{\,\,} \simeq \exp\{-E_A/k_{\rm B}T\}$ , where the corresponding activation energy  $E_A$  was extracted from the STO single crystal measurement presented in Fig. 1(a). The metallic-like behavior of  $G_{\rm IF}$  implies the electronic nature of the charge carriers at the interface since ionic conduction possesses thermal activation (cf. Fig. 1).

From the different pO<sub>2</sub>-dependences of the electrical conductances of the LAO/STO-heterostructure and the STO single crystal, it can be excluded that a mere reduction in the STO substrate during the PLD process is the main reason for the high electron density at the LAO/STO-interface. Reduction would result in mobile oxygen vacancies which would strive for equilibration with the surrounding pO<sub>2</sub> when heating up the samples. Thus, a clear pO2-dependence of the conductivity similar to the behavior of bare STO would be expected for all temperatures above 750 K, since oxygen transport through both the STO crystal and the epitaxial LAO layer has been shown to be possible (see Fig. 1). Moreover, it has been demonstrated that even under high temperature equilibrium conditions the LAO/STO-interface maintains its metallic conductance behavior up to at least 900 K at  $pO_2=10^{-18}$  bar, which even more reflects the fact that the metallic-like interface property does not only result from a reduction in the STO substrate.

Furthermore, it is known from the research on defects in perovskite-type titanates that lanthanum donor doped STO bulk ceramics show a constant conductivity over a broad range of  $pO_2$  in which the charge carrier density is determined by the fixed concentration of ionized dopants. Hence, the weak  $pO_2$ -dependence of the interface conductivity might give hints for localized, donator-type defects in the interface region such as provided by A-site cation intermixing. This is additionally supported by the HAADF image which shows a diffuse interface region extending over 2–3 unit cells. Assuming this scenario of lanthanum doping the sheet carrier density  $n_S$  within the interface region can be estimated directly from the conductance measurements adopting the values for the known electron mobility  $\mu_{STO}$ 

in the STO bulk.<sup>14</sup> Thereby, one obtains  $n_S(850 \text{ K}) = G_{\text{IF}}/e\mu_{\text{STO}} \approx 10^{13} - 10^{14} \text{ cm}^{-2}$  in accordance with published values.<sup>2,4,5,7</sup> For an interface region of width 1 nm, additionally, a donor concentration of [La\*]  $\approx 10^{20} - 10^{21} \text{ cm}^{-3}$  can be estimated corresponding to a La-dopant content of 1–5 at. %. Alternatively, it should be mentioned that also lattice distortions at the interface<sup>15</sup> could give rise to donor-like interface states in analogy to grain boundaries in STO bulk ceramics.<sup>16</sup>

In summary, the results of this study show that for a discussion on the nature of the interface conductivity in LAO/STO heterostructures one has to pay attention that the complex defect chemical state of the entire heterostructure is well defined.

We thank J. Friedrich and M. Gerst for technical support.

<sup>1</sup>A. Ohtomo and H. Y. Hwang, Nature (London) 427, 423 (2004).

<sup>2</sup>S. Thiel, G. Hammerl, A. Schmehl, C. W. Schneider, and J. Mannhart, Science **313**, 1942 (2006).

N. Nakagawa, H. Hwang, and D. Muller, Nature Mater. 5, 204 (2006).
W. Siemons, G. Koster, H. Yamamoto, W. A. Harrison, G. Lucovsky, T. H. Geballe, D. H. A. Blank, and M. R. Beasley, Phys. Rev. Lett. 98, 196802 (2007).

<sup>5</sup>G. Herranz, M. Basletić, M. Bibes, C. Carrétéro, E. Tafra, E. Jacquet, K. Bouzehouane, C. Deranlot, A. Hamzić, J.-M. Broto, A. Barthélémy, and A. Fert, Phys. Rev. Lett. 98, 216803 (2007).

<sup>6</sup>P. R. Willmott, S. A. Pauli, R. Herger, C. M. Schlepütz, D. Martoccia, B. D. Patterson, B. Delley, R. Clarke, D. Kumah, C. Cionca, and Y. Yacoby, Phys. Rev. Lett. **99**, 155502 (2007).

<sup>7</sup>A. S. Kalabukhov, Y. A. Boikov, I. T. Serenkov, V. I. Sakharov, V. N. Popok, R. Gunnarsson, J. Börjesson, N. Ljustina, E. Olsson, D. Winkler, and T. Claeson, Phys. Rev. Lett. **103**, 146101 (2009).

<sup>8</sup>A. Brinkman, M. Huijben, M. van Zalk, J. Huijben, U. Zeitler, J. C. Maan, W. G. van der Wiel, G. Rijnders, D. H. A. Blank, and H. Hilgenkamp, Nature Mater. **6**, 493 (2007).

<sup>9</sup>T. Bieger, J. Maier, and R. Waser, Sens. Actuators B 7, 763 (1992); I. Denk, W. Muench, and J. Maier, J. Am. Ceram. Soc. 78, 3265 (1995).

<sup>10</sup>C. Ohly, S. Hoffmann-Eifert, X. Guo, J. Schubert, and R. Waser, J. Am. Ceram. Soc. 89, 2845 (2006).

<sup>11</sup>D. M. Smyth, *The Defect Chemistry of Metal Oxides* (Oxford University Press, New York, 2000).

<sup>12</sup>R. Waser, J. Am. Ceram. Soc. **74**, 1934 (1991).

<sup>13</sup>T. L. Nguyen, Solid State Ionics **130**, 229 (2000).

<sup>14</sup>R. Moos and K. H. Haerdtl, J. Am. Ceram. Soc. **80**, 2549 (1997).

<sup>15</sup>C. L. Jia, S. B. Mi, M. Faley, U. Poppe, J. Schubert, and K. Urban, Phys. Rev. B **79**, 081405 (2009).

<sup>16</sup>R. A. De Souza, Phys. Chem. Chem. Phys. **11**, 9939 (2009).